

Lattice Boltzmann model for reactive flow simulations

*Original*

Lattice Boltzmann model for reactive flow simulations / DI RIENZO, A.F., Asinari, P., Chiavazzo, E., N. I., P., J., M.. - In: EUROPHYSICS LETTERS. - ISSN 0295-5075. - STAMPA. - 98:(2012), pp. 34001-p1-34001-p6. [10.1209/0295-5075/98/34001]

*Availability:*

This version is available at: 11583/2496261 since:

*Publisher:*

EDP sciences

*Published*

DOI:10.1209/0295-5075/98/34001

*Terms of use:*

This article is made available under terms and conditions as specified in the corresponding bibliographic description in the repository

*Publisher copyright*

(Article begins on next page)

---

# Lattice Boltzmann model for reactive flow simulations

A. F. DI RIENZO<sup>1</sup>, P. ASINARI<sup>1</sup>, E. CHIAVAZZO<sup>1</sup>, N. I. PRASIANAKIS<sup>2</sup> and J. MANTZARAS<sup>2</sup>

<sup>1</sup> *Dipartimento Energia, Politecnico di Torino, Torino 10129, Italy*

<sup>2</sup> *Paul Scherrer Institute, Combustion Research Laboratory, CH-5232 Villigen PSI, Switzerland*

PACS 47.11.-j – Computational methods in fluid dynamics

PACS 47.70.-n – Reactive and radiative flows

PACS 05.20.Dd – Kinetic theory

## Abstract –

In this letter, we propose a lattice Boltzmann (LB) model for reactive flow simulations at the low Mach number regime, which is suitable to accommodate significant density variation. A recently proposed model for compressible thermal flows on standard lattices is herein extended to combustion applications, where species equations are properly described in order to account for compressibility effects. This fundamental extension allows to apply LB approach to a wide range of combustion phenomena, which were not properly addressed so far. The effectiveness of the proposed approach is proved by simulating combustion of hydrogen/air mixtures in a mesoscale channel, and a validation against reference numerical solution in the continuum limit is presented.

---

**Introduction.** – Lattice Boltzmann method (LB) has become a very popular technique for simulating fluid flows [1–6] in a variety of applications such as laminar, turbulent, thermal and multiphase flows, and even beyond hydrodynamics, according to some authors [7]. Reasons for this success are simplicity of implementation, easy handling of complex geometries and suitability for parallel realization. Despite all this, applications of LB to combustion are still limited (see [8] and references therein). One reason is that the original LB recovers Navier-Stokes equations in the incompressible limit, where the density is (approximately) constant. On the contrary, combustion problems exhibit significant density variations due to the heat release in chemical reactions. Therefore, consistent LB models are requested to accurately recover the Navier-Stokes-Fourier equations, coupled to a transport equation for each chemical species. Hence, the numerical model is expected to behave macroscopically like a compressible solver, so as to account for large density and temperature variations.

The first model for combustion simulation was proposed by Succi et al. [9], assuming fast chemistry and cold flames with weak heat release. As a consequence, large density variation was not allowed in the model. Yamamoto et al. [10] presented a model for reactive flows based on the classical incompressible LB formulation [11], under the quite restrictive assumption that the flow field is not affected by chemical reactions. Filippova and Hänel [12] proposed a

scheme for modeling reactive flows at low Mach numbers able to handle density variation. In this model, continuity and momentum equations are solved by means of a modified Bhatnagar-Gross-Krook (BGK) scheme, coupled with finite difference schemes for the solution of energy and species equations. The LB model was derived by modifying the equilibrium populations to have pressure-velocity coupling included in the relaxation step of the distribution function. Macroscopically, this model behaves like a weak-compressible solver. The coupling among continuity, momentum and energy equations is carried out by introducing an additional factor to the rest particle in order to model temporal changes of the density. However, in this way the simplicity of the LB algorithm is somehow lost. Chen et al. [13] overcame this limitation using the model proposed by Guo et al. [14] for the solution of the flow field.

In Ref. [15], an LB model has been introduced with energy conservation on standard lattices. This (consistent) LB model is still limited to weakly compressible flows and is not suitable to accurately simulate thermal flows with large density and temperature variations. However, unlike more traditional approaches, this model makes unnecessary the introduction of a separate population set for the energy field. In Refs. [16] and [17], the consistent LB has been extended to derive a model for simulating compressible thermal flows on standard lattices. The key *ingredient* is introduction of correction terms into

the kinetic Boltzmann-BGK equation, so that the Navier-Stokes-Fourier equations are accurately recovered. In [17] the same model has been tested and validated in case of subsonic flows with large temperature variations, typically encountered in combustion. More specifically, by solving the benchmark problem in [18], this model proved to be a good candidate for simulating reactive flows as it has shown capacity to handle temperature ratios larger than 10.

In this letter, we investigate the suitability of the aforementioned compressible thermal model for the solution of combustion problems. To this purpose, without a lack of generality, we will not consider detailed chemistry, while a global chemical step for hydrogen/air reactive mixtures is used instead. The letter is organized as follows. In Section 1, the governing equations for reactive flows at the low Mach number limit are summarized. In Section 2, the lattice Boltzmann model for simulating reactive flows is presented: the LB scheme for the species equations is described. In Section 3, the LB model for the species transport equation is validated for a one-dimensional problem, for which the analytical solution can be found. The reactive LB model is validated for a *mesoscale* channel [19] against a reference solution obtained by means of FLU-ENT [20]. In Section 4 conclusions are drawn and future works outlined.

**1. Governing Equations.** – Simulation of reactive flows at low Mach number requires the solution of conservation equations for mass, momentum, and energy as follows [21]:

$$\partial_t \rho + \nabla \cdot (\rho \mathbf{u}) = 0, \quad (1a)$$

$$\partial_t (\rho \mathbf{u}) + \nabla \cdot (\rho \mathbf{u} \otimes \mathbf{u} + p \mathbf{I}) = \nabla \cdot \mathbf{\Pi}, \quad (1b)$$

$$\partial_t (\rho h_s) + \nabla \cdot (\rho \mathbf{u} h_s + \mathbf{q}) = \frac{dp}{dt} + \mathbf{\Pi} : \nabla \mathbf{u} - \sum_{k=1}^N h_k^0 \dot{\omega}_k W_k, \quad (1c)$$

$$\partial_t (\rho Y_k) + \nabla \cdot (\rho \mathbf{u} Y_k) - \nabla \cdot (\rho D_k \nabla Y_k) = \dot{\omega}_k W_k, \quad (1d)$$

where  $\rho$  is the mixture density,  $\mathbf{u}$  the mass weighted velocity,  $p$  the pressure,  $\mathbf{\Pi}$  the viscous tensor,  $h_s = c_{p,k} T$  the sensible enthalpy,  $T$  being the mixture temperature and  $c_{p,k}$  the specific heat of the  $k$ -th species ( $k = 1, \dots, N$ ). Fick's law applies to diffusion of chemical species. The mass fraction, the reaction rate, the molecular weight and the enthalpy of formation of the  $k$ -th species are denoted by  $Y_k$ ,  $\dot{\omega}_k$ ,  $W_k$  and  $h_k^0$ , respectively. In Eq. (1c) spatially isobaric assumption has been used. Here, in the heat flux  $\mathbf{q}$ , we neglect the species relative enthalpy flux  $\rho \sum_k Y_k h_k^s \mathbf{V}_k$ , with  $\mathbf{V}_k$  the diffusion velocity of species  $k$ .

**2. Lattice Boltzmann Method for reactive flows.** – LB approach solves a discrete kinetic equation where the main unknowns are the distribution functions of moving particles. Updating these distribution functions requires only informations along fixed directions identified by the lattice velocity  $\mathbf{e}_i$ . According to standard terminology, LB schemes are denoted as  $DdQq$ , meaning that  $q$

particle ensembles move on a  $d$ -dimensional lattice. Eqs. (1a-1c) and Eq. (1d) are recovered in the macroscopic limit by the following kinetic equations with the BGK collision model:

$$g_i(\mathbf{x} + \mathbf{e}_i \delta t, t + \delta t) = g_i(\mathbf{x}, t) + \frac{2\delta t}{\delta t + 2\tau} [f_i^{eq}(\mathbf{x}, t) - g_i(\mathbf{x}, t)] + \frac{2\tau \delta t}{\delta t + 2\tau} [\Psi_i(\mathbf{x}, t) + \Phi_i(\mathbf{x}, t)], \quad (2)$$

$$\xi_{i,k}(\mathbf{x} + \mathbf{e}_i \delta t, t + \delta t) = \xi_{i,k}(\mathbf{x}, t) + \omega_k^{(*)} \left[ \xi_{i,k}^{eq(*)}(\mathbf{x}, t) - \xi_{i,k}(\mathbf{x}, t) \right] + Q_{Y_k}. \quad (3)$$

$\rho$ ,  $\mathbf{u}$  and  $T$  are computed as moments of  $g_i$ , while  $Y_k$  as moment of  $\xi_i$ .  $\Psi$  and  $\Phi$  are the correction terms designed in such a way to properly recover the momentum and energy equations, respectively. The quantity  $\Phi$  also includes the energy source term  $Q_h = -\sum_k h_k^0 \dot{\omega}_k W_k$ . Detailed derivation of the thermal model (2) and its implementation can be found in Refs. [16] and [17]. Below, the LB model for the species equation is discussed. It is worth stressing that the model (2) is based on a fixed heat capacity  $c_p = 2$  in LB units (due to a restriction on the ratio of specific heats,  $\gamma = 2$ , and non-dimensionalisation of the gas constant  $\mathcal{R} = 1$  in LB units). Therefore, the present model for reactive flows inherits this same feature, whereas the latter limitation may be overcome in future works by additional properly designed correction terms.

### 2.1 Lattice Boltzmann model for species equation.

Standard lattice Boltzmann models for combustion (e.g. [13]) emulate advection-diffusion-reaction transport equations by means of the following kinetic equation:

$$\xi_{i,k}(\mathbf{x} + \mathbf{e}_i \delta t, t + \delta t) = \xi_{i,k}(\mathbf{x}, t) + \omega_k \left[ \xi_{i,k}^{eq}(\mathbf{x}, t) - \xi_{i,k}(\mathbf{x}, t) \right] + Q_{Y_k} \quad (4)$$

where  $\xi_{i,k}$  and  $\xi_{i,k}^{eq}$  are the distribution function and the equilibrium distribution functions for species  $k$  along the lattice direction  $i$ , respectively, and  $\omega_k$  is the relaxation frequency.  $Q_{Y_k}$  is the species source term defined as:

$$Q_{Y_k} = \dot{\omega}_k W_k. \quad (5)$$

Both D2Q9 and D2Q5 models can be used to recover the species transport equation. However, here for simplicity, we consider the D2Q5 model, where the equilibrium populations are defined as:

$$\xi_{i,k}^{eq} = w_i \rho Y_k [1 + 3(\mathbf{e}_i \cdot \mathbf{u})], \quad (6)$$

with the lattice weights  $w_0 = 1/3$ ,  $w_i = 1/6$  ( $i = 1, \dots, 4$ ), and the lattice velocities  $\mathbf{e}_0 = (0, 0)$ ,  $\mathbf{e}_i = (\cos(i-1)\pi/2, \sin(i-1)\pi/2)$  ( $i = 1, \dots, 4$ ). The moments corresponding to the equilibrium populations (6) are:

$$\sum_{i=0}^4 \xi_{i,k}^{eq} = \sum_{i=0}^4 \xi_{i,k} = \rho Y_k, \quad (7a)$$

$$\sum_{i=0}^4 e_{i,\alpha} \xi_{i,k}^{eq} = \rho Y_k u_\alpha, \quad (7b)$$

$$\sum_{i=0}^4 e_{i,\alpha}^2 \xi_{i,k}^{eq} = \frac{1}{3} \rho Y_k. \quad (7c)$$

Unfortunately the previous approach fails in case of large density gradients. To the best of our knowledge, some models allow large density variations in the fluid flow, but neglecting the corresponding feedback to the species fields (see, e.g., [13]).

Eq. (4)-(5) recover the species transport equation (1d) with a deviation term:

$$\nabla \cdot (D_k Y_k \nabla \rho), \quad (8)$$

which is activated in case of significant compressibility effects (i.e. large  $\nabla \rho$ ). In order to remove the deviation term in the species equation, two possible strategies may be adopted:

- To introduce in Eq. (4) a correction term to be approximated, e.g., by means of finite difference formulas, consistently with the thermal model described in Refs. [16] and [17];
- To modify the equilibrium population and the relaxation frequency in order to enforce Eq. (4) to accurately recover Eq. (1d).

In this letter, we follow the second strategy, because it only relies upon the LB formulation.

Deviation term (8) stems from the second-order moment. In order to remove it, the first step is to modify the equilibrium distribution function as follows:

$$\begin{aligned} \xi_{0,k}^{eq(*)} &= \rho Y_k \left(1 - \frac{2}{3} \varphi\right), \\ \xi_{1,\dots,4,k}^{eq(*)} &= \frac{1}{6} \rho Y_k (\varphi + 3(\mathbf{e}_i \cdot \mathbf{u})), \end{aligned} \quad (9)$$

where  $\varphi = \rho^{(*)}/\rho$ ,  $\rho^{(*)}$  is a fixed value for the entire domain at any time step, with  $\rho^{(*)}$  being the minimum value of the density field. The moments corresponding to the modified equilibrium (9) are:

$$\sum_{i=0}^4 \xi_{i,k}^{eq(*)} = \sum_{i=0}^4 \xi_{i,k} = \rho Y_k, \quad (10a)$$

$$\sum_{i=0}^4 e_{i,\alpha} \xi_{i,k}^{eq(*)} = \rho Y_k u_\alpha, \quad (10b)$$

$$\sum_{i=0}^4 e_{i,\alpha}^2 \xi_{i,k}^{eq(*)} = \frac{1}{3} \rho^{(*)} Y_k. \quad (10c)$$

The second step for recovering Eq. (1d) consists in redefining the relaxation frequency in Eq. (4). The following relation is proposed:

$$\omega_k^{(*)} = \frac{1}{\frac{1}{2} + \frac{1}{\varphi} \left(\frac{1}{\omega_k} - \frac{1}{2}\right)}, \quad (11)$$

$\delta x$	Error $L^2[Y]$	Slope
0.05	$2.745521 \times 10^{-2}$	–
0.025	$8.186644 \times 10^{-3}$	1.75
0.0125	$2.495928 \times 10^{-3}$	1.71

Table 1: Convergence analysis of the LB model for the species equations in the case of diffusive scaling ( $\delta t \sim \delta x^2$ ).

such that, if  $\varphi = 1$  then  $\omega_k^{(*)} = \omega_k$ . In both D2Q5 and D2Q9 models the relaxation frequency  $\omega_k$  is related to the  $k$ -th species mass diffusivity  $D_k$  in Eq. (1d) as:

$$D_k = \frac{1}{3} \left(\frac{1}{\omega_k} - \frac{1}{2}\right). \quad (12)$$

With the suggested modification, Eq. (3) recovers Eq. (1d) in the macroscopic limit. It is clear from Eq. (11) that, for stability reasons,  $\varphi < 1$ . It is worth stressing that, in the proposed model, there is a single consistent density field which is the one coming from populations  $g_i$  (2), and can thus properly accommodate large density variations. Therefore here, compressibility is taken into account using the  $g_i$  populations for computing density, which is in turn adopted in both the equilibrium populations (9) and the relaxation frequency (11) (through  $\varphi$ ): In this way, density variations are consistently introduced in the species equations (3) (asymptotically recovering Eq. (1d)).

Without a lack of generality, a minimal lattice D2Q5 is used for the species transport equations (unlike the hydrodynamic part (2) which is based on a D2Q9 lattice). Such a choice is motivated by convenience in reducing the memory demand. This is particularly desirable in the case of detailed chemical kinetics, where a large number of species is typically taken into account. To this respect, the comparative study performed below provides numerical evidence that this choice is feasible. However, for the sake of completeness, we report below the equilibrium populations in the case a D2Q9 lattice is adopted for the species transport equations:

$$\begin{aligned} \xi_{0,k}^{eq(*)} &= \frac{1}{9} \rho Y_k (9 - 5\varphi), \\ \xi_{1,\dots,4,k}^{eq(*)} &= \frac{1}{9} \rho Y_k (\varphi + 3(\mathbf{e}_i \cdot \mathbf{u})), \\ \xi_{5,\dots,8,k}^{eq(*)} &= \frac{1}{36} \rho Y_k (\varphi + 3(\mathbf{e}_i \cdot \mathbf{u})). \end{aligned} \quad (13)$$

**3. Numerical results.** – First, validation of the proposed LB model for the species transport equation is discussed in this section. The 1D non-dimensional form of Eq. (1d) at the steady state for one species ( $k = 1$ ) non-reacting flow with constant mass diffusivity is:

$$\rho' u'_x \frac{dY}{dx'} = \frac{D'}{ReSc} \frac{d}{dx'} \left( \rho' \frac{dY}{dx'} \right), \quad (14)$$

where  $x' = x/L_0$ ,  $\rho' = \rho/\rho_0$ ,  $u'_x = u_x/u_0$  and  $D' = D/(u_0 L_0)$ , with 0 and ' denoting the reference and the

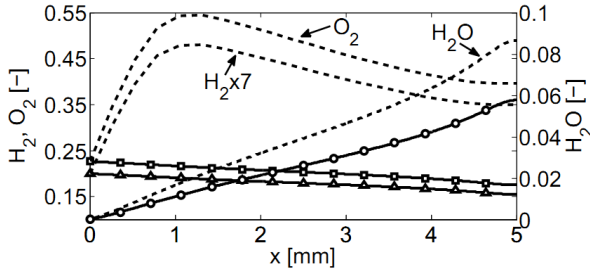


Fig. 1: Species mass fractions along the channel walls predicted by basic model (4) (dashed-lines) are compared to those recovered by the proposed model (solid-lines). Symbols are the reference solution (circles  $\text{H}_2\text{O}$ , squares  $\text{O}_2$ , triangles  $\text{H}_2$ ). Present application is Test 1 described in Section 3.

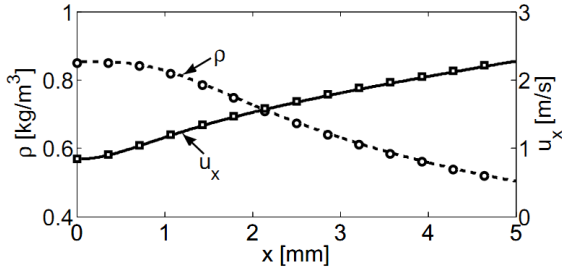


Fig. 2: Test 1: Mixture density and velocity along the horizontal plane of symmetry. Solid lines and symbols represent the LB and the reference solutions, respectively.

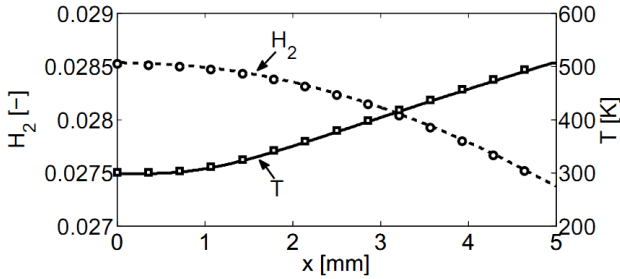


Fig. 3: Test 1: Mixture temperature and  $\text{H}_2$  mass fraction along the horizontal plane of symmetry. Solid lines and symbols represent the LB and the reference solutions, respectively.

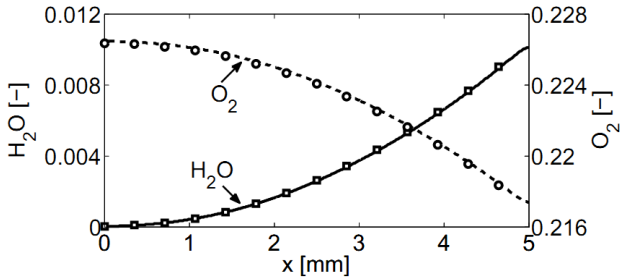


Fig. 4: Test 1:  $\text{H}_2\text{O}$  and  $\text{O}_2$  mass fractions along the horizontal plane of symmetry. Solid lines and symbols represent the LB and the reference solutions, respectively.

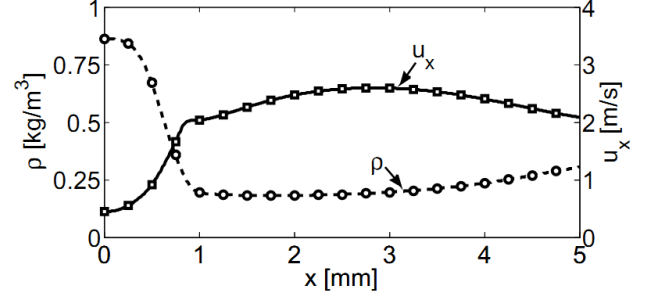


Fig. 5: Test 2: Mixture density and x-velocity component along the horizontal plane of symmetry. Solid lines and symbols represent the LB and the reference solutions, respectively.

non-dimensional quantities, respectively.  $Re$  and  $Sc$  are the Reynolds number and the Schmidt number. Defining  $Z = dY/dx'$  and  $\Lambda = \rho'Z$ , Eq. (14) is rewritten as:

$$u'_x \Lambda = \frac{D'}{ReSc} \frac{d\Lambda}{dx'}. \quad (15)$$

Imposing  $u' = 1/\Lambda$ , the solution of Eq. (15) is:

$$\Lambda = x' \frac{ReSc}{D'} + \Lambda_0, \quad (16)$$

where  $\Lambda_0$  is an arbitrary constant. The condition  $d(\rho'u'_x)/dx' = 0$  is satisfied imposing  $\rho' = \Lambda$ , such that  $Z = 1$ . Thus, the analytical solution of Eq. (14) is:

$$Y_{an} = x' + Y_0, \quad (17)$$

which can be used to validate the proposed LB model for species transport equation. Here, periodicity is assumed in the  $y$ -direction of a square domain, so as to reduce the problem to 1D. Analytical solution is imposed at the inlet ( $x' = 0$ ) and the outlet ( $x' = 1$ ) of the domain. The  $L^2$  norm of deviation of numerical results from the exact solution are reported in Table 1, in case of diffusive scaling (i.e.  $\delta t \sim \delta x^2$ ) [22].

In order to validate the LB model for reactive flows, we consider combustion of stoichiometric premixed hydrogen/air reactive mixture between two parallel horizontal plates, with a fixed length-to-height aspect ratio,  $L/h = 2.5$  and length  $L = 5$  mm. This domain is usually referred to as mesochannel [19]. Ignition of the reactive mixture is produced and sustained by heated walls. For fixed values of the channel height  $h$  and the wall temperature, different types of flames are observed, as function of the inlet velocity  $U_{in}$  [19]. Validation of the present LB model is carried out for  $U_{in} = 0.85$  m/s (Test 1) and  $U_{in} = 0.48$  m/s (Test 2). In both cases, constant temperature  $T_{in} = 300$  K is prescribed at the inflow and a well premixed stoichiometric  $\text{H}_2$ -air mixture enters from the inlet. Along the channel walls, zero-flux for all species (e.g. chemically inert walls) and no-slip conditions for both velocity component are imposed. The wall temperature is prescribed via a hyperbolic tangent connecting

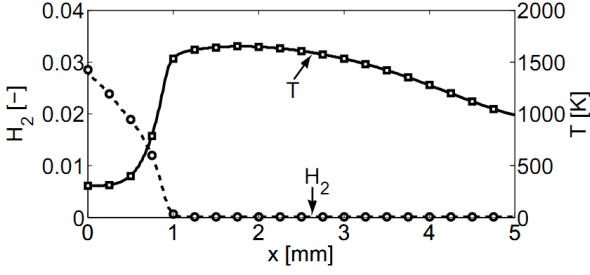


Fig. 6: Test 2: Mixture temperature and  $H_2$  mass fraction along the horizontal plane of symmetry. Solid lines and symbols represent the LB and the reference solutions, respectively.

fresh conditions up to the highest temperature  $T_w = 960\text{K}$ , according to  $T(x) = S_1 \tanh(\beta x - \gamma) + (T_w - S_1)$ , with  $S_1 = 330\text{K}$ ,  $\beta = 5$ ,  $\gamma = 4.2$  with  $x$  expressed in millimeters. Such profile mimics heat losses at the channel inlet due to convective cooling of the cold incoming flow and radiative heat losses to the colder surroundings. At the outlet, atmospheric pressure and zero Neumann boundary conditions are imposed. For the sake of simplicity, we have assumed  $D_k = D$  and  $c_{p,k} = c_p$  for the mass diffusivity and specific heat of all chemical species. The global reaction  $H_2 + 1/2 O_2 \rightarrow H_2O$  by Marinov et al. [23] is employed for the evaluation of the reaction rates in Eqs. (1c) and (1d):

$$R = AC_{H_2}C_{O_2}^{0.5} \exp\left(-\frac{E}{RT}\right), \quad (18)$$

with  $A = 1.8 \times 10^{13} \text{ mol}^{-0.5} \text{ cm}^{1.5} \text{ s}^{-1}$  and  $E = 146.4 \text{ kJ/mol}$ .

For validation purposes, solutions of the LB scheme have been compared against solutions from FLUENT [20]. In this simulation we make use of  $501(N_x) \times 201(N_y)$  regular lattice. Mixture properties have been assumed constant: the specific heat is  $c_p = 1.4 \text{ kJ/(kgK)}$ , the kinematic viscosity is  $\nu = 0.22 \times 10^{-4} \text{ m}^2/\text{s}$ , the mass diffusivity  $D = 1.4 \times 10^{-4} \text{ m}^2/\text{s}$ , the Prandtl number  $\text{Pr} = 0.465$  and the Lewis number  $Le = \alpha/D = 1/3$ , where  $\alpha$  is thermal diffusivity. Concerning the flow field, diffusive boundary conditions [24] are used for the walls, while equilibrium populations are imposed at the inlet and outlet as follows:

$$g_i^{in}(l=1, m) = f_i^{eq}\left(\frac{p(l=2, m)}{T^{in}}, \mathbf{u}^{in}, T^{in}\right), \quad (19)$$

$$g_i^{out}(l=N_x, m) = f_i^{eq}\left[\frac{p^{out}}{T(l=N_x-1, m)}, \mathbf{u}(l=N_x-1, m), T(l=N_x-1, m)\right], \quad (20)$$

where indices  $l$  and  $m$  denote the nodes along  $x$ - and  $y$ -directions, respectively, with  $p^{out}$  being the LB outlet pressure corresponding to  $p = 1 \text{ atm}$ .

For the species equations, bounce-back is applied at the walls while equilibrium populations are used at the inlet and outlet as follows:

$$\xi_{i,k}^{in}(l=1, m) = \xi_{i,k}^{eq}(\rho^{in} Y_k^{in}, \mathbf{u}^{in}), \quad (21)$$

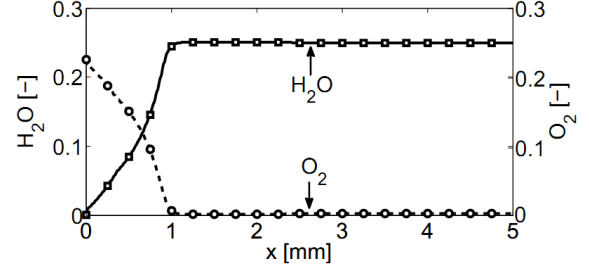


Fig. 7: Test 2:  $H_2O$  and  $O_2$  mass fractions along the horizontal plane of symmetry. Solid lines and symbols represent the LB and the reference solutions, respectively.

$$\xi_{i,k}^{out}(l=N_x, m) = \xi_{i,k}^{eq}\left[(\rho Y_k)^{out}, \mathbf{u}(l=N_x, m)\right], \quad (22)$$

where  $Y_k^{in}$  represents the mass fraction of the fresh mixture, while  $\rho^{in} = p(l=2, m)/T^{in}$ ,  $\mathbf{u}(l=N_x, m) = \mathbf{u}(l=N_x-1, m)$  and

$$(\rho Y_k)^{out} = \frac{3}{2}\rho(l=N_x-1, m)Y_k(l=N_x-1, m) - \frac{1}{2}\rho(l=N_x-3, m)Y^k(l=N_x-3, m). \quad (23)$$

Eqs. (19) ensure first-order accurate homogeneous Neumann condition for pressure at the inlet while, owing to (20), same boundary condition holds for velocity and temperature at the outlet. Finally, Eqs. (22) and (23) mimic free outlet condition for  $\rho Y_k$  though extrapolation over nodes with  $l=N_x-3$  and  $l=N_x-1$ .

The proposed reactive LB model is validated against reference solutions from FLUENT for both test problems. In Figs. 2-7, comparisons between our results and the reference ones are reported at steady state. Good agreement is demonstrated. In Figs. 2-4, the solutions for  $U_{in} = 0.85 \text{ m/s}$  are presented. In this case, a longer channel is needed, in order to have complete fuel conversion. However, a smaller channel length has been chosen for validation purposes, so to reduce the computational effort. In order to check the suitability of the model at larger temperature ratios in the bulk, the velocity at the inlet is reduced to  $U_{in} = 0.48 \text{ m/s}$ . In this case, a closed symmetric flame is anchored at the vicinity of the inlet and fully converts the fuel within the channel (Figs. 5-7). In the test problems, the maximum relative difference between solutions are found to be: 2% for the density, 4.2% for the velocity, 5.7% for the temperature, and 3% for the chemical species. In order to check the consistency of the LB scheme, we computed the following quantities for the H, O and N elements:

$$M_n = \int_0^h \sum_{k=1}^N \rho u_x Y_k c_{k,n} dy, \quad (24)$$

where  $c_{k,n}$  is the number of atoms of the  $n$ -th element in the  $k$ -th species. Mass conservation is verified by measuring the previous quantities through the domain. For

Test 1,  $M_H = 8.01 \times 10^{-5} \pm 5 \times 10^{-6}$ ,  $M_O = 6.42 \times 10^{-4} \pm 9.42 \times 10^{-6}$  and  $M_N = 2.11 \times 10^{-3} \pm 3.96 \times 10^{-5}$ . For Test 2,  $M_H = 8.26 \times 10^{-5} \pm 1.73 \times 10^{-6}$ ,  $M_O = 5.15 \times 10^{-5} \pm 7.4 \times 10^{-7}$  and  $M_N = 3.17 \times 10^{-4} \pm 1.96 \times 10^{-9}$ . We finally stress that mass conservation through (24) is accurate at the same level as FLUENT solution.

**4. Conclusions.** – In this letter, we introduce a lattice Boltzmann scheme for simulating reactive flows in the low Mach number limit, on the basis of a recently proposed thermal model. **The latter method enables to handle significant density and temperature variations without loss of numerical stability and with good accuracy.**

Moreover, the thermal model had to be coupled with mass conservation equations for the chemical species. For this case, a model able to deal with compressibility effects was also derived. To this purpose, we proposed a new scheme for solving the advection-diffusion equation of chemical species, where compressibility effects are taken into account by modifying both the equilibrium distribution function and the relaxation frequency in the BGK collision term. This fundamental extension allows to apply LB approach to a wide range of combustion phenomena, which were not properly addressed so far.

The present model for reactive flows has been validated against a reference code in the continuum limit for hydrogen/air reactive mixture, **by simulating two different test problems.** Solutions of the proposed model are found to be in **very good** agreement with the reference results.

Here, a global step mechanism with only three reactive species has been used. Simulation of reactive flows with detailed chemistry by means of lattice Boltzmann method, poses a challenge due to large number of fields needed to store in memory (compared to a conventional method). Moreover, stiffness imposes small time steps, making the computational effort even more demanding. From this point of view, model reduction techniques represent a possible solution, where both stiffness and the number of fields involved in the computations are drastically reduced [25, 26].

## REFERENCES

- [1] F. J. Higuera, S. Succi, R. Benzi, Lattice Gas Dynamics with Enhanced Collisions, *EuroPhys. Lett.*, 1989, 9, 345-39
- [2] F. J. Higuera, J. Jimenez, Boltzmann approach to lattice gas simulations, *EuroPhys. Lett.*, 1989, 9, 663-668
- [3] H. Chen, S. Chen, H. W. Matthaeus, Recovery the Navier-Stokes equations using lattice gas Boltzmann method, *Phys. Rev. A*, 1992, 45, R5339-R5342
- [4] Y. Qian, D. d’Humières, P. Lallemand, Lattice BGK models for Navier-Stokes equation, *Europhys. Lett.*, 1992, 17, 479-484
- [5] X. He, L. S. Luo, Theory of lattice Boltzmann method: from the Boltzmann equation to the lattice Boltzmann equation, *Phys. Rev. E*, 1997, 56, 6811-6817
- [6] S. Succi, The lattice Boltzmann equation for fluid dynamics and beyond, 2nd ed. Oxford University Press, New York, 2001
- [7] M. Sbragaglia, S. Succi, A note on the lattice Boltzmann method beyond the Chapman-Enskog limits, *Europhys. Lett.*, 2006, 73 (3), 370-376
- [8] C. E. Frouzakis, Lattice Boltzmann Methods for Reactive and Other Flows, in *Turbulent Combustion Modeling* edited by T. Echekki and E. Mastorakos, Fluid Mechanics and Its Applications, 2011, 95, Part 4, 461-486
- [9] S. Succi, G. Bella, F. Papetti, Lattice kinetic theory for numerical combustion, *J. Sci. Comp.*, 1997, 12, 395-408
- [10] K. Yamamoto, X. He, G. D. Doolen, Simulation of combustion field with lattice Boltzmann method, *J. Stat. Phys.*, 2002, 107, 367-383
- [11] Q. Zou, S. Hou, S. Chen, G. D. Doolen, An improved incompressible lattice Boltzmann model for time-independent flows, *J. Stat. Phys.*, 1995, 81, 35-48
- [12] O. Filippova, D. Hänel, A novel lattice BGK approach for low Mach number combustion, *J. Comp. Phys.*, 2000, 158, 139-160
- [13] S. Chen, Z. Liu, Z. Tian, B. Shi., C. Zheng, A simple lattice Boltzmann scheme for combustion simulation, *Comp. Math. Appl.*, 2008, 55, 1424-1432
- [14] Z. L. Guo, B. C. Shi, N. C. Wang, Lattice BGK model for incompressible Navier-Stokes equation, *J. Comp. Phys.*, 2000, 165, 288-306
- [15] S. Ansumali, I. V. Karlin, Consistent Lattice Boltzmann method, *Phys. Rev. Lett.*, 2005, 95, 260605-260608
- [16] N. I. Prasianakis and I.V. Karlin, Lattice Boltzmann method for simulation of thermal flows on standard lattices, *Phys. Rev. E*, 2007, 76, 016702-016712
- [17] N. I. Prasianakis, I. V. Karlin, Lattice Boltzmann method for simulation of compressible flows on standard lattices, *Phys. Rev. E*, 2008, 78, 016704-016710
- [18] A. G. Tomboulides, S. A. Orzag, A quasi-two dimensional benchmark problem for low Mach number compressible codes, *J. Comp. Phys.*, 1998, 146, 691-706
- [19] G. Pizza, C. E. Frouzakis, J. Mantzaras, A. G. Tomboulides, K. Boulouchos, Dynamics of premixed hydrogen/air flames in mesoscale channels, *Comb. Flame*, 2008, 155, 2-20
- [20] Fluent Inc., Fluent Release 6. 3 User Guide, Fluent Inc. (2006)
- [21] C. K. Law, Combustion Physics, Cambridge University Press, 2006
- [22] M. Junk, A. Klar, L. S. Luo, Asymptotic analysis of the lattice Boltzmann equation, *Journ. Comp. Phys.*, 2005, 210, 676-704
- [23] N. M. Marinov, C. K. Westbrook, W. J. Pitz, Detailed global chemical kinetics model for hydrogen, *8th Int. Symp. on Transport Properties*, 1995, San Francisco, CA
- [24] S. Ansumali, I. V. Karlin, Kinetic boundary condition for the lattice Boltzmann method, *Phys. Rev. E*, 2002, 66, 026311-026316
- [25] E. Chiavazzo, I. V. Karlin, A. N. Gorban, K. Boulouchos, Combustion simulation via lattice Boltzmann and reduced chemical kinetics, *J. Stat. Mech.*, 2009, P06013
- [26] E. Chiavazzo, I. V. Karlin, A. N. Gorban, K. Boulouchos, Coupling of the model reduction technique with the lattice Boltzmann method for combustion simulations, *Comb. Flame*, 2010, 157, 1833-1849